

MATHEMATICAL MODELLING OF WATER FLOW IN PAPER PRESS MACHINES ¹

R. ČIEGIS, M. MEILŪNAS and A. ŠTIKONAS

Vilnius Gediminas Technical University

Saulėtekio al. 11, LT-10223 Vilnius, Lithuania

E-mail: {rc, mm, ash}@fm.vtu.lt

Received November 4, 2004; revised December 8, 2004

Abstract. In this work, mathematical models of wet pressing of paper are studied. Our goal is to compare two mathematical models, which are developed for simulation of filtration processes in paper press machines. Both models were obtained from the same general model of the compressible porous medium, but different assumptions were used. Modified models are developed that describe water losses at the boundaries of the porous layer and the importance of this factor is investigated. Numerical algorithms are developed for simulation of the liquid movement in the deformable porous media. It is proved that the discrete problem is stable if the time step τ satisfies the inequality $\tau \leq Ch^2$. It follows from the stability analysis that the mathematical model describes an ill-posed problem for some values of parameters used in simulations.

Key words: porous media, modelling, drying of paper, finite-volume algorithms

1. Introduction

The flow of fluid in porous materials occurs in a number of industrial applications such as drying of wood and paper, soil mechanics, liquid composite moulding (see [2, 5, 6, 7, 10, 14]). Many mathematical models are developed for the analysis of such processes. In this work, models of wet pressing of paper are investigated. Our goal is to compare two mathematical models, which were developed for simulation of filtration processes in paper press machines. Both models were obtained from the same general model of the compressible porous medium, but different assumptions were used.

In the paper of Velten and Best [14] it is assumed that water is moving only in one dimension along the felt. They investigated the development and

¹ This work was supported by the Lithuanian State Science and Studies Foundation within the framework of the Eureka project OPTPAPER EU-2623, E-2002.02.27

dynamics of the full saturation zones in the porous material. We note that "no flow" boundary conditions across the porous layer were used.

In the paper of Hiltunen [9] (see also [10]) two liquid phases are taken into account, i.e. the air phase is added to the model. Contrary to [14] it is assumed that the velocity of the water along the felt coincides with the solid phase velocity and the movement of water across the porous material is investigated. The effect of saturation is neglected in [9], therefore the pressure equation is simplified seriously.

In Section 2 we formulate a general model of the compressible porous medium. Evolution of fully saturated zones is investigated in Section 3. We propose a modification of the model, which was used in [14], and investigate the impact of water losses to the dynamics of the saturation zones. A three phase model of a paper press machine is investigated in Section 4. The main goal of this section is to construct a discrete approximation of the system of PDE and to investigate the stability of the obtained finite-volume scheme.

2. A General Model of the Compressible Porous Medium

In conventional paper machine a porous layer (paper web) is compressed either between two rotating rolls or between a rotating roll and a fixed surface (a pressing shoe). The porous layer is partially filled with a fluid. The mixture theory is used to describe the flow of fluids in deformable porous materials. In this section we present general governing equations, which are used to simulate the processes in paper press machines. Good introductions into mathematical models describing drying of paper are given in [9, 14].

Let us consider a sample of volume element V of a mixture in porous layer. It consist of three phases: fluid and air phases indexed "f" and "a", and a solid phase, which consists of fibrous solid material and is indexed "s". As always we assume the size of this volume element is large compared with the size of pores and small compared with the size of the entire system. We denote the volumes occupied by water, air and solid material by V_f, V_a and V_s respectively. The *volume fraction* of each component is defined by:

$$\phi_\alpha = \frac{V_\alpha}{V}, \quad \alpha = f, a, s.$$

Due to volume conservation the following constraint should be satisfied:

$$\phi_f + \phi_a + \phi_s = 1, \quad (2.1)$$

thus it is sufficient to write two equations for determination of two volume fractions of the mixture. The porosity ϕ of the porous material is defined by

$$\phi = 1 - \phi_s.$$

Mass conservation of three constituents

Assuming that the solid and fluid phases are intrinsically incompressible, (i.e., the intrinsic densities of the solid $\tilde{\rho}_s$ and fluid $\tilde{\rho}_f$ are constant), we obtain the local mass conservation equations in the Eulerian framework:

$$\frac{\partial \phi_\alpha}{\partial t} + \nabla \cdot (\phi_\alpha \mathbf{v}_\alpha) = 0, \quad \alpha = s, f. \quad (2.2)$$

Since the air is a compressible liquid, we get the following equation:

$$\frac{\partial}{\partial t} (\phi_a \tilde{\rho}_a) + \nabla \cdot (\phi_a \tilde{\rho}_a \mathbf{v}_a) = 0.$$

Treating the air as an ideal gas, we obtain the equation of state for the gas phase:

$$\tilde{\rho}_a = \frac{1}{C_p} \tilde{p}_a,$$

Thus the mass conservation equation of the air phase is given by

$$\frac{\partial}{\partial t} (\phi_a \tilde{p}_a) + \nabla \cdot (\phi_a \tilde{p}_a \mathbf{v}_a) = 0. \quad (2.3)$$

Considering the slow flow regime and ignoring the weak time-dependent effects, we obtain the mass balance equations in the stationary case

$$\begin{cases} \nabla \cdot (\phi_\alpha \mathbf{v}_\alpha) = 0, & \alpha = s, f, \\ \nabla \cdot (\phi_a \tilde{p}_a \mathbf{v}_a) = 0. \end{cases} \quad (2.4)$$

Momentum balance equations

We will not consider general momentum balance equations. To focus on flows in porous media, the simplifying assumptions are used. Considering the slow liquid flow and assuming that excess interaction forces between the solid and liquids are proportional to the velocity differences $\mathbf{v}_\alpha - \mathbf{v}_s$, $\alpha = a, f$, we write the general momentum balance equations as (see [1]):

$$\phi_\alpha (\mathbf{v}_\alpha - \mathbf{v}_s) = -\frac{\mathbf{K}_\alpha}{\mu_\alpha} \nabla \tilde{p}_a, \quad \alpha = a, f, \quad (2.5)$$

where μ_α are the viscosity coefficients and \mathbf{K}_α are the permeability tensors. Equations (2.5) are the three-phase flow Darcy law for the case of moving porous medium.

The permeability coefficients $\mathbf{K}_\alpha = \mathbf{K}_\alpha(\phi, S)$ depend on the porosity ϕ of the porous material and the saturation S of water, where S is defined by

$$S = \frac{\phi_f}{\phi}.$$

Different models are used to describe the permeability of the porous medium (see, [9, 14]) and they generalize the well-known Kozeny–Carman equation [3].

External forces

The rolls exert large forces on the liquid and solid phases. These forces are taken into account by using the classical Terzaghi principal as discussed in [14]. It is noted in [9] that for highly compressible porous materials the Terzaghi principal may not be applicable and instead of it a more general form should be used.

To connect the Terzaghi principal with the other equations of the model of multiphase flow in the deformable porous medium, it is necessary to specify a model for the deformation of the porous material. In most papers the viscoelastic model is used.

In the following sections we consider two examples of simplified models, which are obtained from this general equations.

3. Evolution of Fully Saturated Zones

It is stated in [14] that evolution of a fully saturated zone critically determines the effectiveness of the drying process. For example, the press felts need to be unsaturated in some part of the rolling zone, in order to be able to take up significant amount of water from the paper.

The mathematical model is developed in [14], which is based on two-phase flow equations in one dimension. It is used to predict the evolution of fully saturated regions and to estimate the sizes of the saturation region [14].

We note that "no flow" boundary conditions are used for fluid phase in this model. Our goal is to generalize the model in order to include water losses and to consider the dynamics of the saturation under various scenarios of water losses.

3.1. Formulation of the model

It is assumed that a porous layer is moving in the positive x direction. The following basic assumptions are used to simplify the multidimensional equations of mass conservation (2.4) and momentum balance (2.5):

- The y direction (following the roll axes) is neglected since the rolls are up to 10 m long.
- The water flow in the z direction is neglected.
- The air phase is neglected, i.e. it is assumed that $\phi_a = 0$, $p_a = 0$.

Mass conservation of the fluid

We consider the flow regime in the region:

$$D = \{ (x, z) : x_a \leq x \leq x_b, A(x) \leq z \leq B(x) \},$$

where $A(x), B(x)$ are the lower and upper boundaries of the porous layer, respectively. Let $d(x) = B(x) - A(x)$ be the thickness of the porous layer.

Since we consider the mass flux only in the x direction, then taking a small volume $[x, x + h]$ we can write the discrete mass balance equation

$$-d\phi_f v_f|_{x+h} + d\phi_f v_f|_x = hJ,$$

where J estimates water losses through the lower and upper boundaries of the volume element. If "no flow" boundary conditions are assumed, then $J = 0$.

Dividing both sides of the equation by h and taking the limit $h \rightarrow 0$, we obtain the one-dimensional mass conservation equation:

$$-(d\phi_f v_f)' = J. \quad (3.1)$$

We note that $J = 0$ is taken in [14].

A different mass balance equation can be obtained if apriori assumptions are changed. For example, let us consider a case, when the derivative of the flux in the x direction does not depend on the remaining coordinate z . Then integrating the stationary mass conservation equation (2.4) in the region

$$\Delta D = \{ (x, z) : x_1 \leq x \leq x_2, \quad x_2 = x_1 + h, \quad A(x) \leq z \leq B(x) \}$$

we get

$$\int_{x_1}^{x_2} \int_{A(x)}^{B(x)} \frac{\partial}{\partial x} (\phi_f v_f) dz dx + \int_{x_1}^{x_2} (\phi_f v_{zf})|_{A(x)}^{B(x)} dx = 0.$$

The term

$$J_1 = \frac{1}{h} \int_{x_1}^{x_2} (\phi_f v_{zf})|_{A(x)}^{B(x)} dx$$

defines water losses (or increment) through the lower and upper surfaces of the finite-volume. Using the assumption given above and integrating the first integral by parts we get a discrete mass conservation equation

$$-(d\phi_f v_f)|_{x_2} + (d\phi_f v_f)|_{x_1} + \int_{x_1}^{x_2} d' \phi_f v_f dx = hJ_1.$$

Taking the limit $h \rightarrow 0$ gives the differential mass conservation equation

$$-(d\phi_f v_f)' + d' \phi_f v_f = J_1.$$

The Darcy law

Momentum balance equation (2.5) becomes

$$\phi_f (v_f - v_s) = -\frac{K_f}{\mu_f} \frac{dp_f}{dx}, \quad (3.2)$$

where v_f, v_s and $K_f(\phi, S)$ are real valued functions depending on the x argument.

Substituting (3.2) into mass conservation equation (3.1) we obtain a convection – diffusion equation for unknown $p_f(x)$

$$-\left(d \frac{K_f}{\mu_f} p_f'\right)' + (d \phi_f v_s)' = -J.$$

We note that in [14] a factor d is omitted in the first term on the left-hand side of this equation.

The obtained equation also depends on S and ϕ_f . Additional constitutive relations are used to close the system. By using the definition of the saturation we express ϕ_f as $\phi_f = S \phi$.

From experiments we know the relation between capillary pressure $p_c = p_a - p_f$ and saturation S (see, e.g. [1])

$$S = \tilde{g}(p_c).$$

In our case $p_a = 0$, therefore we obtain the needed relation $S = g(p_f)$.

Substituting these expressions into the convection – diffusion equation we get the nonlinear differential equation in the unknown $p_f(x)$:

$$-\left(d \frac{K_f(\phi, g(p_f))}{\mu_f} p_f'\right)' + (d \phi g(p_f) v_s)' = -J. \quad (3.3)$$

Boundary conditions were defined in [14] as follows:

$$p_f(-x_b) = g^{-1}(S_0), \quad d \frac{K_f}{\mu_f} p_f' \Big|_{x=x_b} = 0,$$

where x_b is some large number, such that no influence of x_b on the solution p_f is observed.

Constitutive relations

Since our goal is to investigate the influence of water losses on the saturation dynamics, we use the same parametrized function $g(p_f)$ as in [14]

$$g(p_f) = \begin{cases} \frac{1}{\frac{1}{1-s_\infty} + \left(\frac{p_f}{a}\right)^n} + s_\infty, & p_f \leq 0, \\ 1, & p_f > 0, \end{cases}$$

where parameters s_∞, a, n were selected to fit the experimental data. The obtained saturation – pressure function $g(p_f)$ is shown in Fig. 1a.

A constitutive relation for K_f is expressed as a nonlinear function of porosity and saturation (see [14]):

$$K_f(\phi, S) = k_0 \frac{\phi^3}{1 - \phi^2} S^{3.4}, \quad (3.4)$$

where k_0 is the permeability factor.

We note that in [9, 10] a similar but different expression was used to describe this nonlinear function

$$K_f(\phi, S) = k_0 \frac{\phi^3}{(1 - \phi)^2} S^{3.4}. \quad (3.5)$$

In the case of full saturation of water, (3.5) reduce to the widely used empirical Kozeny – Carman equation, which relates porosity and permeability. Nevertheless, in order to compare our results with [14], we have used formula (3.4) in all numerical experiments.

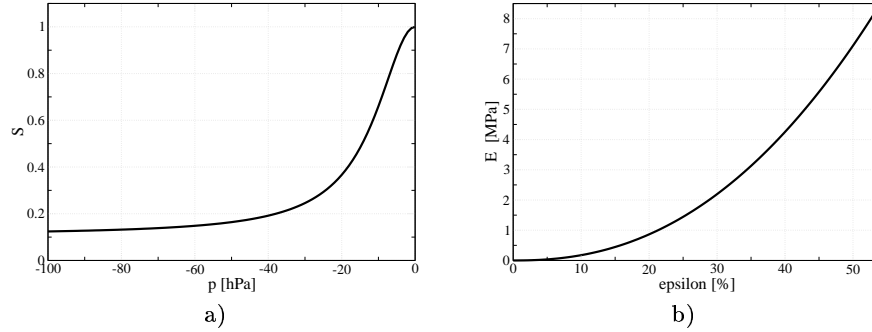


Figure 1. a) Saturation – pressure function: $s_\infty = 0.11$, $a = -1.2$, $n = 2$, b) press – strain function.

Model for the deformation of porous material

Let assume that we know the function $d(x)$, which describes the thickness of the porous layer, and let d_0 be the thickness of the uncompressed porous layer. The volume $V(x)$ of the element of porous material is proportional to $d(x)$. Let denote by $V_s(x) = C d_s(x)$ the volume occupied by the solid phase. Assuming that the solid phase is not deformed and only the pore space is compressed, we get the equality

$$d_s(a) = d_s(x).$$

Dividing it by d_0 and rearranging some terms we obtain the equation

$$1 - \phi_0 = (1 - \phi(x)) \frac{d(x)}{d_0},$$

from which the porosity $\phi(x)$ can be computed

$$\phi(x) = 1 - \frac{d_0}{d(x)} (1 - \phi_0).$$

The following model was proposed in [14] to determine $d(x)$ in the deformed felt. Function $d = d(x; d_{min})$ expresses the thickness of the porous layer as a function of x and the minimum distance between the roll surfaces d_{min} :

$$d(x; d_{min}) = \begin{cases} d_0, & x \leq x_l(d_{min}) = -\sqrt{R^2 - \left(\frac{1}{2}(d_0 - d_{min}) - R\right)^2}, \\ 2R + d_{min} - 2\sqrt{R^2 - x^2}, & x_l(d_{min}) \leq x \leq x_r(d_{min}). \end{cases}$$

In the first interval the porous material is uncompressed, in the second one it follows the geometry of the roll surfaces until stress τ_{zz} becomes zero at $x = x_r(d_{min})$. The nonlinear Kelvin – Voigt law is used to take into account viscoelasticity of the felt:

$$\tau_{zz}(x) = E(x) + v_s \Lambda \frac{d}{dx} E(x),$$

where Λ is a viscoelastic time constant. The stress – strain function E is fitted to data given in [14]:

$$E(\epsilon) = 35\epsilon^{2.3} \text{ [MPa]}.$$

The obtained function is shown in Fig. 1b.

For $x > x_r(d_{min})$ the strain $\epsilon = \epsilon(x; d_{min}) = 1 - d(x; d_{min})/d_0$ is determined from $E(x)$, which satisfies the initial value problem

$$\begin{cases} \frac{d}{dx} E(x) = -\frac{1}{v_s \Lambda} E(x), \\ E(x_r(d_{min})) = E(\epsilon(x_r; d_{min}); d_{min}). \end{cases} \quad (3.6)$$

Thus we get:

$$d(x; d_{min}) = d_0(1 - \epsilon(x)), \quad x > x_r(d_{min}).$$

The parameter d_{min} is obtained from the Terzaghi equation. The forces F_f and F_s can be computed as

$$F_f(d_{min}) = \int_{x_l(d_{min})}^{x_r(d_{min})} p_f dx, \quad F_s(d_{min}) = \int_{x_l(d_{min})}^{x_r(d_{min})} \left(E(x; d_{min}) + v_s \Lambda \frac{d}{dx} E(x; d_{min}) \right) dx,$$

therefore we get the nonlinear equation for d_{min} :

$$\int_{x_l(d_{min})}^{x_r(d_{min})} \left(p_f + E(x; d_{min}) + v_s \Lambda \frac{d}{dx} E(x; d_{min}) \right) dx = F. \quad (3.7)$$

3.2. Discretization of the model

Let us introduce the uniform grid

$$\omega_h = \{x_i : x_i = -x_b + ih, i = 0, 1, \dots, N, x_N = x_b\}.$$

In the following we will denote the discrete approximations of continuous functions using a subscript "h", e.g. the pressure function p_f will be approximated by the function

$$p_{f,hi} = p_{f,h}(x_i) = p_{f,h}(x_i, d_{min}).$$

The hydrostatic pressure function is defined as follows:

$$\tilde{p}_h = Sp_f + (1 - S)p_a.$$

Iterative algorithm for solving equation (3.7)

Approximating integrals in (3.7) by the trapezoidal rule

$$S_h(d_{min}) = \sum_{i=n_L+1}^{n_R} \frac{p_{hi} + p_{h,i-1} + E(\epsilon_{hi}) + E(\epsilon_{h,i-1})}{2} h + v_s \Lambda \left(E(\epsilon_{h,n_R}) - E(\epsilon_{h,n_L}) \right),$$

we get the discrete nonlinear equation

$$S_h(d_{min}) - F = 0.$$

The obtained nonlinear equation can be solved by many iterative algorithms. Since function S_h is monotonical, we use the bisection method to find d_{min} .

Finite volume scheme for solving the pressure equation

During each bisection iteration (or *outer* iteration) we should solve a nonlinear problem, which approximates the boundary value problem for the pressure function.

Let us introduce the following notation of finite differences:

$$\delta_- p_{hi} = \frac{p_{hi} - p_{h,i-1}}{h}, \quad \delta_+ p_{hi} = \frac{p_{h,i+1} - p_{h,i}}{h}.$$

Applying the finite-volume method we approximate equation (3.3) and boundary conditions by the following conservative finite-difference scheme (see [6])

$$\begin{cases} -a_{i+\frac{1}{2}}(p_h) \delta_+ p_{hi} + a_{i-\frac{1}{2}}(p_h) \delta_- p_{hi} + w_i g(p_{hi}) - w_{i-1} g(p_{h,i-1}) = -J_i h, \\ p_{h0} = g^{-1}(S_0), \quad a_{N-\frac{1}{2}}(p_h) \delta_- p_{hN} = 0, \end{cases}$$

where we use notation

$$a_i(p_h) = d(x_i) \frac{K_f(\phi_{hi}, g(p_{hi}))}{\mu_f}, \quad w_i = d(x_i) \phi_{hi} v_s.$$

Since we are interested in monotonous approximations, the convection term is approximated by upwinding formula. Therefore the total truncation error of the discretization is only of order $\mathcal{O}(h)$. The accuracy of the obtained solution is estimated *a posteriori* by using the Runge rule.

The nonlinear discrete problem is linearized by the following iterative algorithm:

$$\begin{cases} -a_{i+\frac{1}{2}}(p_h^s) \delta_+ p_{hi}^{s+1} + a_{i-\frac{1}{2}}(p_h^s) \delta_- p_{hi}^{s+1} + w_i g'(p_{hi}^s) p_{hi}^{s+1} \\ \quad - w_{i-1} g'(p_{h,i-1}^s) p_{h,i-1}^{s+1} = -w_i g(p_{hi}^s) + w_{i-1} g(p_{h,i-1}^s) \\ \quad + w_i g'(p_{hi}^s) p_{hi}^s - w_{i-1} g'(p_{h,i-1}^s) p_{h,i-1}^s - J_i h, \\ p_{h0}^{s+1} = g^{-1}(S_0), \quad a_{N-\frac{1}{2}}(p_h^s) \delta_- p_{hN}^{s+1} = 0. \end{cases}$$

3.3. Computational experiments

In numerical examples we take parameters and coefficients from [14]. The water viscosity μ_f was set to 4.7×10^{-4} Pa s. In the expression for the relative permeability K_f , the factor k_0 was set to $k_0 = 10^{-10} m^2$. The viscoelastic time constant Λ was set to 0.0004 s. The parameters of paper machine and porous layer were taken as

$$d_0 = 2.5 \text{ mm}, \quad R = 100 \text{ cm}, \quad F = 70 \text{ kN/m}, \quad S_0 = 0.5, \quad \phi_0 = 0.52.$$

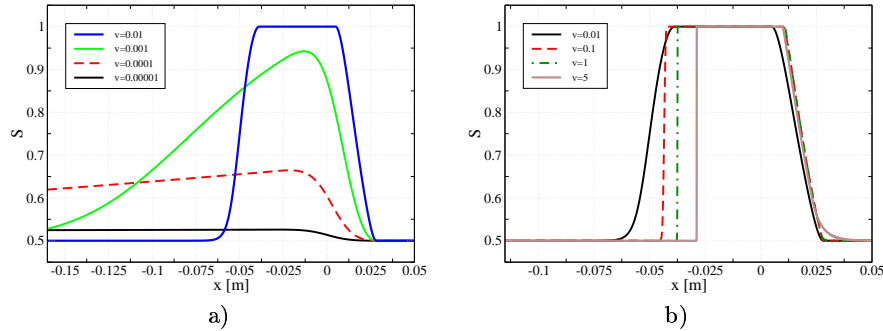


Figure 2. Saturation profiles for different solid velocities: a) $1 \times 10^{-5} \leq v_s \leq 0.01$, b) $0.01 \leq v_s \leq 5$.

First, following analysis presented in [14], we assume that "no flow" boundary conditions are valid, i.e. $J = 0$. The saturation of water profiles for solid phase velocities between $v_s = 0.0001$ and $0.1 m/s$ are shown in Fig. 2a. The full saturation $S = 1$ zone arises only at sufficiently large solid phase velocity.

For small velocities the pressure profiles are close to the constant pressure p_{f0} (see equation (3.3) for $J = 0$ and v_s small) and saturation profiles are very smooth.

Our results are different from results presented in [14], where it is stated that for small solid velocities the water amount practically remains unchanged at each point of porous material and therefore the saturation increases around the center of the rolling zone at $x = 0$, reflecting the decrease of the porosity ϕ in the rolling zone. Such profiles can not be obtained from the presented mathematical model, since the pressure remains almost constant, therefore the water amount should be redistributed according the saturation – pressure equation.

Our main goal of this section is to include water losses into the formulation of the mathematical model and to consider the dynamics of the saturation under various scenarios of water losses. We assume that water losses take place mostly at the center of the rolling zone (see [9]) and describe it as

$$J(x) = J_0 \phi_f(x) S(x) \epsilon(x).$$

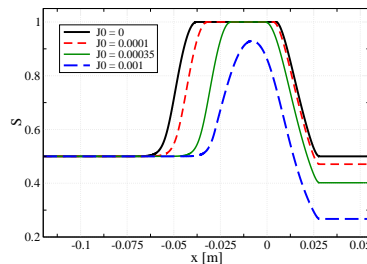


Figure 3. Saturation profiles for different solid velocities.

We have fixed the solid phase velocity to $v = 1$ m/s and simulated the process for different values of J_0 . The obtained saturation profiles are shown in Fig. 3. We see, that for sufficiently intensive water losses the saturated zones disappear. It is interesting to note that about 50 percents of water is taken away for $J_0 = 0.001$. It agrees well with results presented in [9], where full saturation of water is not considered in the mathematical model.

4. Three Phase Model of Paper Press Machine

In this section we consider the mathematical model, which was proposed by Hiltunen [9].

4.1. Formulation of the model

The following main assumptions are assumed to be valid:

- Time – dependent effects are small and can be neglected.
- The y direction (following the roll axes) is neglected since the rolls are up to 10 m long.
- The flow of both liquids, i.e. water and air, is purely transversal in the rest frame of the mat entering the nip. This means that

$$v_\alpha^x = v_s^x, \quad \alpha = a, f.$$

We will use simple notations of velocities

$$c = v_s^x, \quad v_\alpha = v_\alpha^z, \quad \alpha = a, f, s.$$

In the press section of a paper machine, water is squeezed out of the paper web into the felt, thus we consider the flow in the following region $D = D_w \cup D_f$, where D_w, D_f are the paper web and felt regions, respectively:

$$D_f = \left\{ (x, z) : -\frac{L}{2} \leq x \leq \frac{L}{2}, \quad -\gamma_f(x) \leq z \leq 0 \right\},$$

$$D_w = \left\{ (x, z) : -\frac{L}{2} \leq x \leq \frac{L}{2}, \quad 0 \leq z \leq \gamma_w(x) \right\}.$$

With these assumptions we get from (2.4), (2.5) the following mass balance equations

$$\begin{cases} c \frac{\partial \phi_\alpha}{\partial x} + \frac{\partial}{\partial z} (\phi_\alpha v_\alpha) = 0, & \alpha = s, f, \\ c \frac{\partial}{\partial x} (\phi_a \tilde{p}_h) + \frac{\partial}{\partial z} (\phi_a \tilde{p}_h v_a) = 0, \end{cases} \quad (4.1)$$

and the momentum balance equations

$$\begin{cases} \phi_\alpha (v_\alpha - v_s) = -\frac{K_\alpha}{\mu_\alpha} \frac{\partial \tilde{p}_h}{\partial z}, & \alpha = a, f, \\ \frac{\partial p_s}{\partial z} - \tilde{p}_h \frac{\partial \phi_s}{\partial z} = \frac{\phi_a^2 \mu_a}{K_a} (v_a - v_s) + \frac{\phi_f^2 \mu_f}{K_f} (v_f - v_s). \end{cases} \quad (4.2)$$

Summing up all equations of (4.2), we get that

$$\frac{\partial p_T}{\partial z} = 0,$$

where the total pressure is defined as

$$p_T = p_a + p_f + p_s = p_s + (1 - \phi_s) \tilde{p}_h.$$

Using the generalized Terzaghi principle we write the pressure balance equation in a form

$$p_T(x) = p_{st}(s) + f(\phi_s(x, z)) \tilde{p}_h(x, z), \tag{4.3}$$

where $s = 1 - \frac{\phi_{s0}}{\phi_s}$ is the strain and p_{st} is the structural pressure in the absence of hydrostatic pressure. It is noticed in [9] that porous material can show hysteresis and suffer permanent deformation, hence the structural pressure is parametrized as

$$p_{st} = p_{st0} \frac{r}{1-r}, \quad r = \begin{cases} \frac{s}{s_0}, & \text{during compression,} \\ \frac{s - \varepsilon s_m}{s_0 - \varepsilon s_0}, & \text{during expansion,} \end{cases} \tag{4.4}$$

where s_m is the maximum strain achieved by a certain point.

It remains to get the equation for the solid phase velocity v_s . Summing up all three mass conservation equations (4.1) we get the first order differential equation for v_s :

$$\frac{\partial}{\partial z} (\phi_f u_f + \phi_a u_a + v_s) = -\frac{\phi_a}{\tilde{p}_h} \left(c \frac{\partial \tilde{p}_h}{\partial x} + (u_a + v_s) \frac{\partial \tilde{p}_h}{\partial z} \right),$$

where $u_\alpha = v_\alpha - v_s$, $\alpha = f, a$. Using the relation (4.3) and the mass conservation equation for the solid phase we convert the x -derivative of the hydrostatic pressure into the known x -derivative of the total pressure:

$$\left(1 + \frac{\phi_a}{\tilde{p}_h} \phi_s q\right) \frac{\partial v_s}{\partial z} = -\frac{\phi_a}{\tilde{p}_h} \left(\frac{c}{f(\phi_s)} \frac{\partial p_T(x)}{\partial x} - q u_a \frac{\partial \phi_s}{\partial z} \right) - \frac{\partial}{\partial z} (\phi_f u_f + \phi_a u_a), \tag{4.5}$$

where

$$q = \frac{\tilde{p}_h f'(\phi_s) + p'_{st}(\phi_s)}{f(\phi_s)}.$$

The gradient of the hydrostatic pressure is assumed to be constant in the felt

$$\frac{\partial \tilde{p}_h(x, z)}{\partial z} = \frac{\Delta \tilde{p}_h}{\gamma_f(x)}, \quad (x, z) \in D_f, \tag{4.6}$$

where $\Delta \tilde{p}_h$ is the total pressure drop across the felt.

Boundary and continuity conditions

On the surface of the upper roll

$$\Gamma_w = \left\{ (x, z) : -\frac{L}{2} \leq x \leq \frac{L}{2}, \quad z = \gamma_w(x) \right\},$$

we assume that "no flow" boundary conditions are valid

$$v_\alpha = v_s, \quad \alpha = a, f, \quad (x, z) \in \Gamma_w. \tag{4.7}$$

On the lower surface

$$\Gamma_f = \left\{ (x, z) : -\frac{L}{2} \leq x \leq \frac{L}{2}, z = \gamma_f(x) \right\}$$

the hydrostatic pressure is given and the water and air move freely out of the felt:

$$\tilde{p}_h(x, z) = \tilde{p}_{hf}.$$

The web – felt interface Γ_{wf}

$$\Gamma_{wf} = \left\{ (x, z) : -\frac{L}{2} \leq x \leq \frac{L}{2}, z = 0 \right\}$$

is fixed, therefore

$$v_s = 0, \quad (x, z) \in \Gamma_{wf}.$$

The water and air flows are assumed to be continuous on the interface Γ_{wf} .

4.2. Discretization of the model

In this section we present a finite–volume scheme for solving the described above mathematical model of paper press machine.

We define discrete meshes which are dynamically adapted to the moving boundary of the solid phase. The mesh in x -dimension is given by

$$\omega_\tau = \left\{ x^n : x^n = x^{n-1} + \tau^{n-1}, \quad n = 1, 2, \dots, N, \quad x^0 = -\frac{L}{2}, \quad x^N = \frac{L}{2} \right\}.$$

The mesh in z -direction is also non-uniform and it depends on the position of boundaries γ_f and γ_w :

$$\omega_h(x^n) = \left\{ z_j^n : z_j^n = z_{j-1}^n + h_{j-1}^n, \quad j = -J/2, \dots, J/2 \right\},$$

where

$$z_{-J/2}^n = -\gamma_f^n, \quad z_0^n = \gamma_{wf}^n, \quad z_{J/2}^n = \gamma_w^n.$$

Here and in the following we use the notation $u_j^n = u(x^n, z_j)$ for any discrete function u .

Let assume that the solution is known for $x = x^n$, i.e. discrete functions $\phi_s^n, \phi_f^n, v_s^n, v_f^n, z^n$ are given. The finite–volume discretization is defined by the following main steps of the algorithm.

1. Determination of the mesh ω_h^{n+1} .

In the web region the nodes at t^{n+1} are defined as

$$z_j^{n+1} = z_j^n + \tau^n \frac{v_{sj}^n}{c}, \quad j = 1, 2, \dots, J/2. \quad (4.8)$$

In the felt region and at the web–felt interface the nodes are not moving:

$$z_j^{n+1} = z_j^0, \quad j = -J/2, \dots, 0.$$

2. Discrete mass conservation equation for solid fraction.

Since grid nodes are moving with velocity v_s , the solid volume fraction values are given by

$$\begin{aligned}\phi_{sj}^{n+1} &= \phi_{sj}^n \frac{h_j^n + h_{j-1}^n}{h_j^{n+1} + h_{j-1}^{n+1}}, \quad -J/2 < j < J/2, \\ \phi_{s,-J/2}^{n+1} &= \phi_{s,-J/2}^n \frac{h_{-J/2}^n}{h_{-J/2}^{n+1}}, \quad \phi_{s,J/2}^{n+1} = \phi_{s,J/2}^n \frac{h_{J/2-1}^n}{h_{J/2-1}^{n+1}}.\end{aligned}\quad (4.9)$$

3. Discrete mass conservation equation for water fraction.

Numerical methods for solving equations describing the fluid flow problems in a moving coordinate system are presented in many papers, see [4, 11, 12]. Here we will apply the discretization method, which was used in [6]. First we obtain the integral formulation of the mass balance equation

$$c \frac{\partial \phi_f}{\partial x} + \frac{\partial}{\partial z} (\phi_f v_f) = 0.$$

Integrating it in the elementary volume $[z_s(x), z_f(x)]$ and using the equality

$$\frac{d}{dx} \int_{z_s(x)}^{z_f(x)} \phi_f(x, z) dz = \int_{z_s(x)}^{z_f(x)} \frac{\partial \phi_f}{\partial z} dz + \frac{dz_f(x)}{dx} \phi_f(x, z_f(x)) - \frac{dz_s(x)}{dx} \phi_f(x, z_s(x)),$$

gives the integral mass balance equation

$$c \frac{d}{dx} \int_{z_s(x)}^{z_f(x)} \phi_f(x, z) dx + f_f(x) - f_s(x) = 0, \quad (4.10)$$

where

$$f_\alpha(x) = [v_f(x, z_\alpha(x)) - v_s(x, z_\alpha(x))] \phi_f(x, z_\alpha(x)).$$

Taking elementary volume $[z_{j-\frac{1}{2}}(x), z_{j+\frac{1}{2}}(x)]$ and applying the finite-volume method we approximate the integral equation (4.10) by the following conservative explicit finite-difference scheme

$$\frac{h_{j-\frac{1}{2}}^{n+1} \phi_{fj}^{n+1} - h_{j-\frac{1}{2}}^n \phi_{fj}^n}{\tau^n} + F(w_{j+\frac{1}{2}}^n, \phi_{f,j+1}^n, \phi_{fj}^n) - F(w_{j-\frac{1}{2}}^n, \phi_{fj}^n, \phi_{f,j-1}^n) = 0,$$

where the numerical flux $F(w_{j+\frac{1}{2}}, \phi_{j+1}, \phi_j)$ is defined as follows [6]:

$$\begin{aligned}F(w_{j+\frac{1}{2}}, \phi_{j+1}, \phi_j) &= \frac{1}{2} w_{j+\frac{1}{2}} (\phi_{j+1} + \phi_j) - \frac{1}{2} |w_{j+\frac{1}{2}}| (\phi_{j+1} - \phi_j), \\ w_{j+\frac{1}{2}}^n &= v_{f,j+\frac{1}{2}}^n - v_{s,j+\frac{1}{2}}^n, \quad h_{j-\frac{1}{2}}^n = \frac{h_j^n + h_{j-1}^n}{2}.\end{aligned}$$

The boundary conditions are approximated by

$$\frac{h_{-\frac{j}{2}}^{n+1} \phi_{f,-\frac{j}{2}}^{n+1} - h_{-\frac{j}{2}}^n \phi_{f,-\frac{j}{2}}^n}{2\tau^n} + F \left(w_{-\frac{j}{2}+\frac{1}{2}}^n, \phi_{f,-\frac{j}{2}+1}^n, \phi_{f,-\frac{j}{2}}^n \right) - \tilde{F}_{-\frac{j}{2}}^n = 0,$$

$$\frac{h_{\frac{j}{2}-1}^{n+1} \phi_{f,\frac{j}{2}}^{n+1} - h_{\frac{j}{2}-1}^n \phi_{f,\frac{j}{2}}^n}{2\tau^n} - F \left(w_{\frac{j}{2}-\frac{1}{2}}^n, \phi_{f,\frac{j}{2}}^n, \phi_{f,\frac{j}{2}-1}^n \right) = 0,$$

where $\tilde{F}_{-\frac{j}{2}}^n$ defines the "free out-flow" and "no-inflow" flux:

$$\tilde{F}_{-\frac{j}{2}}^n = \begin{cases} 0, & \text{if } w_{-\frac{j}{2}}^n > 0, \\ w_{-\frac{j}{2}}^n \phi_{f,-\frac{j}{2}}^n, & \text{if } w_{-\frac{j}{2}}^n \leq 0. \end{cases}$$

The saturation of water fraction should always satisfy the conditions

$$0 \leq S_{fj}^{n+1} \leq 1, \quad z_j \in \omega_h(x^{n+1}).$$

Therefore, after finding ϕ_f^{n+1} from the discrete mass balance equation, an artificial limiter is additionally applied:

$$\phi_{fj}^{n+1} := \begin{cases} \phi_{fj}^{n+1}, & \text{if } 0 \leq S_{fj}^{n+1} \leq 1, \\ S_{fj}^{n+1} \phi_j^{n+1}, & \text{otherwise.} \end{cases}$$

3. New values of the air fraction.

The new values of the air fraction are obtained from (2.1)

$$\phi_{aj}^{n+1} = 1 - \phi_{sj}^{n+1} - \phi_{fj}^{n+1}, \quad z_j \in \omega_h(x^{n+1}). \quad (4.11)$$

4. The hydrostatic pressure equation.

The new values of the hydrostatic pressure are obtained from (4.3)

$$\tilde{p}_{hj}^{n+1} = \frac{p_T(x^{n+1}) - p_{st,j}^{n+1}}{f(s_j^{n+1})}, \quad z_j \in \omega_h(x^{n+1}), \quad (4.12)$$

where the structural pressure is computed from (4.4)

$$p_{st,j}^{n+1} = p_{st0} \frac{r_j^{n+1}}{1 - r_j^{n+1}}.$$

5. The new values of relative velocities.

The new values of velocities relative to the solid phase are obtained from the Darcy law:

$$\phi_{\alpha j}^{n+1} u_{\alpha j} = -\frac{K_{\alpha j}^{n+1}}{\mu_{\alpha}} \frac{p_{h,j+1}^{n+1} - p_{hj}^{n+1}}{h_j^{n+1}}, \quad \alpha = a, f, \quad z_j \in \omega_h(x^{n+1}).$$

6. The new values of all velocities.

Velocity of the solid phase v_s^{n+1} is obtained by solving a discretized equation (4.5). Then the water and air velocities are given by

$$v_{\alpha j}^{n+1} = v_{sj}^{n+1} + u_{\alpha j}^{n+1}, \quad \alpha = a, f, \quad z_j \in \omega_h(x^{n+1}).$$

In this model the pressure equation is solved explicitly (we note, that in the previous model the pressure equation was global in x -direction). Such simplification of the model was possible due to two assumptions:

- The pressure is deformation driven and only the difference between the total pressure (which does not depend on z) and the structural pressure is taken into account.
- The flow is purely transversal.

The constitutive relation between the saturation and capillary pressure is not used in the model to close the system, thus gradients in the initial distribution of the saturation are not smoothed by the pressure. For example, let us assume that the porous mat is not compressed $p_T(x) = 0$ and the following initial conditions are valid:

$$v_s^0 = 0, \quad v_f^0 = 0, \quad v_a^0 = 0, \quad \phi_{aj}^0 = 0, \quad \phi_{sj}^0 = 0.3, \quad z_j \in \omega_h(x^0),$$

$$\phi_{fj}^0 = \begin{cases} 0.6 & \text{if } j = j_0, \\ 0.3 & \text{if } j \neq j_0. \end{cases}$$

Then the water distribution remains unchanged for any $x^n \in \omega_\tau$, i.e. $\phi_f^n = \phi_f^0$.

4.3. Stability analysis

In this subsection we consider the stability of the obtained finite-volume approximation. In [9] the stability analysis is done separately for each equation. Since mass conservation equations (4.9) and (4.10) are hyperbolic, we get that explicit approximations are stable if discrete steps τ^n satisfy the following estimates

$$v_s^n \tau^n < \min_j h_j^n, \quad v_f^n \tau^n < \min_j h_j^n.$$

We note that such analysis is not sufficient in order to prove the stability of the system of equations. Let consider a simplified model of two-phase flow, which is described by the mass conservation equations

$$\begin{cases} \frac{\partial \phi_s}{\partial x} + \frac{\partial}{\partial z}(\phi_s v_s) = 0, \\ \frac{\partial \phi_f}{\partial x} + \frac{\partial}{\partial z}(\phi_f v_f) = 0, \end{cases}$$

and the Darcy equation

$$\phi_f(v_f - v_s) = -\frac{K_f}{\mu_f} \frac{\partial \tilde{p}_h}{\partial z}.$$

Summing up mass conservation equations we get that

$$\frac{\partial}{\partial z}(\phi_s v_s + \phi_f v_f) = 0,$$

or

$$v_s + \phi_f(v_f - v_s) = C,$$

where C is a constant. Taking into account the Darcy equation, we get the mass balance equation of the solid phase

$$\frac{\partial \phi_s}{\partial x} + C \frac{\partial \phi_s}{\partial z} = -\frac{\partial}{\partial z} \left(\phi_s \frac{K_f}{\mu_f} \frac{\partial \tilde{p}_h}{\partial z} \right). \quad (4.13)$$

It was shown above that the hydrostatic pressure is defined as a function $\tilde{p}_h = P(\phi_s)$. If $P' < 0$, we get from (4.13) a parabolic equation

$$\frac{\partial \phi_s}{\partial x} + C \frac{\partial \phi_s}{\partial z} = \frac{\partial}{\partial z} \left(\phi_s \frac{K_f}{\mu_f} |P'(\phi_s)| \frac{\partial \phi_s}{\partial z} \right). \quad (4.14)$$

Then the algorithm presented above is equivalent to discretization of (4.14) by the explicit Euler scheme

$$\frac{\phi_s^{n+1} - \phi_s^n}{\tau} + C \partial_{z,h} \phi_s^n = \partial_{z,h} \left(\phi_s \frac{K_f}{\mu_f} |P'(\phi_s^n)| \partial_{z,h} \phi_s^n \right),$$

where $\partial_{z,h}$ defines a finite-difference operator. It follows from the maximum principle (see [13]) that this scheme is stable only if

$$\tau \leq c \min_j h_j^2.$$

If $P' > 0$, then the proposed mathematical model (4.13) becomes ill-conditioned (similar to so-called heat-conduction equation with the inverse direction of time)

$$\frac{\partial \phi_s}{\partial x} + C \frac{\partial \phi_s}{\partial z} = -\frac{\partial}{\partial z} \left(\phi_s \frac{K_f}{\mu_f} P'(\phi_s) \frac{\partial \phi_s}{\partial z} \right).$$

and special numerical methods should be used to find its solution [8]. For example, the hydrostatic pressure function from (4.3)

$$\tilde{p}_h(x, z) = \frac{p_T(x) - p_s(s)}{1 - \phi_s(x, z)}$$

was used in numerical experiments presented in [9]. In Figure 4 the graphic of this function is presented, when

$$x = 0, \quad p_T(x) = \frac{5}{2} \left(1 + \cos \left(\frac{2\pi x}{L} \right) \right).$$

We see that for $s \in [0.25, 0.35]$ the hydrostatic pressure grows up, leading to an ill-posed problem. There is no experimental data that such a phenomena was observed experimentally.

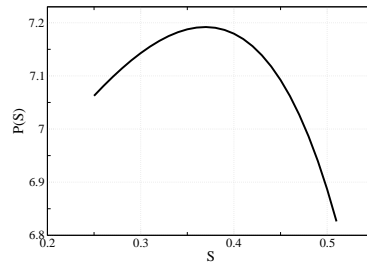


Figure 4. The hydrostatic pressure function for $x = 0$.

References

- [1] M. Allen, G. Behie and J. Trangenstein. *Multiphase flow in porous media*. Springer, Berlin, 1988.
- [2] D. Ambrosi and L. Preziosi. Modelling injection moulding processes with deformable porous preforms. *SIAM J. Appl. Math.*, **61**, 22 – 42, 2000.
- [3] J. Bear and A. Verruijt. *Modeling ground water flow and pollution*. Reidel, Dordrecht, 1987.
- [4] J.P. Boris and D.L. Book. Flux corrected transport. I. SHASTA. A fluid transport algorithm that works. *J. Comp. Physics*, **11**, 39 – 69, 1973.
- [5] R. Čiegis and O. Iliev. Numerical algorithms for modeling of liquid polymer moulding. *Mathematical modelling and analysis*, **8**(3), 181 – 202, 2003.
- [6] R. Čiegis, O. Iliev, S. Rief and K. Steiner. On modelling and simulation of different regimes for liquid polymer moulding. *Computational Methods in Applied Mathematics*, **4**(2), 131 – 162, 2004.
- [7] R. Čiegis, V. Starikovičius and A. Štikonas. Parameters identification algorithms for wood drying modeling. In: A. Buikis, R. Ciegis and A.D. Fitt(Eds.), *Mathematics in Industry-ECMI Subseries, Vol.5, Progress in Industrial Mathematics at ECMI2002*, Springer, Berlin Heidelberg New York, 107 – 112, 2004.
- [8] H.W. Engl, M. Hanke and A. Neubauer. *Regularization of Inverse Problems*. Kluwer, Dondrecht, 1996.
- [9] K. Hiltunen. *Mathematical and numerical modelling of consolidation processes in paper machines, Report 66*. University of Jyväskylä, Department of Mathematics, 1995.
- [10] M. Kataja, K. Hiltunen and J. Timonen. Flow of water and air in a compressible porous medium. a model of wet pressing of paper. *J. Phys. D: Appl. Phys.*, **25**, 1053 – 1063, 1992.
- [11] R.J. LeVeque. *Numerical Methods for Conservation Laws*. Birkhäuser Verlag, 1991.

- [12] P.L. Roe. Some contributions to the modeling of discontinuous flows. *Lect. Notes Appl. Math.*, **22**, 163 – 193, 1985.
- [13] A.A. Samarskii. *The theory of difference schemes*. Marcel Dekker, Inc., New-York, Basel, 2001.
- [14] K. Velten and W. Best. Rolling of unsaturated materials: evolution of a fully saturated zone. *Physical Review E*, **62**(3), 3891 – 3899, 2000.

Vandens srautų popieriaus preso mašinoje matematinis modeliavimas

R. Čiegis, M. Meilūnas, A. Štikonas

Darbe nagrinėjami drėgmės išspaudimo iš popieriaus matematiniai modeliai. Šiame straipsnyje palyginti du matematiniai modeliai, kurie naudojami modeliuoti filtracijos procesus popieriaus preso mašinoje. Abu modeliai išvedami iš tų pačių bendrųjų spūdziosios poringosios terpės modelių, tačiau naudojamos skirtingos prielaidos. Straipsnyje pasiūlytas patikslintas modelis, kuris aprašo vandens ištekimą poringosios terpės sluoksnio krašte, ir ištirta šio faktoriaus įtaka skysčio judėjimui. Pasiūlyti skaitiniai algoritmai skysčio judėjimo poringoje terpėje modeliavimui. Įrodyta, kad tiriant diskrečiojo uždavinio stabilumą neužtenka nagrinėti tik hiperbolinį pernešimo lygčių artinį, o reikia įvertinti ir slėgio lygčių poveikį. Parodyta, kad diskretusis uždavinys yra stabilus, jeigu diskretizacijos pagal laiką žingsnis tenkina sąlygą $\tau \leq Ch^2$. Iš stabilumo analizės išplaukia, kad prie kai kurių modelio parametrų reikšmių modelis aprašo nekorektišką uždavinį.